Electricity trading based on distribution locational marginal price

Zhenhao Li [a], Chun Sing Lai [a,b,*], Xu Xu [c], Zhuoli Zhao [a] and Loi Lei Lai [a]

[a] Department of Electrical Engineering, School of Automation, Guangdong University of Technology, Guangzhou, 510006, China
[b] Brunel Institute of Power Systems, Department of Electronic & Computer Engineering, Brunel University London, London, UB8 3PH, UK
[c] Department of Electrical Engineering, The Hong Kong Polytechnic University, Hong Kong, SAR China
[*] Corresponding email: chunsing.lai@brunel.ac.uk
First and second authors contribute equally

***Abstract*— This paper proposes a novel day-ahead power market for distribution systems. Based on the linearized AC power flow model, the distribution locational marginal price for coupled active and reactive power can be calculated and decomposed into five components, i.e. 1) energy price; 2) loss price caused by nodal active power; 3) loss price caused by nodal reactive power; 4) congestion price and 5) voltage support price, which can provide price signals for distributed generator and aggregator in a distribution system to respond. The energy hub at different nodes can trade with each other and optimize their profit based on distribution locational marginal prices. Game theory is applied to solve the energy trading payment problem. The energy trading problem is decomposed into two subproblems, i.e. operation cost minimization problem and trading payment bargaining problem. The effectiveness and validity of the proposed method are illustrated with a modified IEEE 33-bus system.**

***Index Terms*—Distribution locational marginal price, day-ahead market, energy hub, electricity trading.**

NOMENCLATURE

Variables and Functions:

P_i, Q_i	Nodal active, reactive power at node *i*
PL_{ij}, QL_{ij}	Active, reactive power flow from node *i* to node *j*
PL_l, QL_l	Active, reactive power flow of line *l*
P, Q	Nodal active, reactive power matrix
V, θ	Nodal voltage, angle matrix
$SF_{v-p}, SF_{\theta-p}, SF_{p-p}, SF_{q-p}$	Sensitivity matrix of nodal voltage, angle, active and reactive power magnitude changes *w.r.t.* nodal active power injections
$SF_{v-q}, SF_{\theta-q}, SF_{p-q}, SF_{q-q}$	Sensitivity matrix of nodal voltage, angle, active and reactive power magnitude changes *w.r.t.* nodal reactive power injections
LF_{p-p}, LF_{q-p}	Sensitivity matrix of system active and reactive power loss magnitude changes *w.r.t.* nodal active power injections.
LF_{p-p}, LF_{q-p}	Sensitivity matrix of system active and reactive power loss magnitude changes *w.r.t.* nodal reactive power injections
V_l	Voltage of start bus of line *l*
F_i^p, F_i^q	Factitious nodal demand (FND) of active and reactive power at node *i*
$PLoss$, $QLoss$	Total active and reactive power loss
P_i^G, Q_i^G	Active and reactive power output of generator at node *i*
Q_i^{SVC}, Q_i^{CB}	Reactive power output of static VAr compensator (SVC), capacitor banks (CB) at node *i*

L	Lagrange function of the model
$\sigma_{P,i}^{t}, \sigma_{Q,i}^{t}$	Active and reactive power price at node *i* at time slot *t*
$\sigma_{k}^{p}, \sigma_{k}^{q}$	DLMP for active, reactive power at iteration *k*
$\sigma_{E,k}^{p}, \sigma_{E,k}^{q}$	Energy price for nodal active, reactive power at iteration *k*
$\sigma_{Lp,k}^{p}, \sigma_{Lp,k}^{q}$	Active, reactive power loss price *w.r.t.* nodal active power at iteration *k*
$\sigma_{Lq,k}^{p}, \sigma_{Lq,k}^{q}$	Active, reactive power loss price *w.r.t.* nodal reactive power at iteration *k*
$\sigma_{Con,k}^{p}, \sigma_{Con,k}^{q}$	Congestion price for active, reactive power at iteration *k*
$\sigma_{Vs,k}^{p}, \sigma_{Vs,k}^{q}$	Voltage support price for active, reactive power at iteration *k*
$P_{pur,e,i,DSO}^{t}, P_{pur,g,i,DSO}^{t}$	Electricity and gas purchased from distribution system operator (DSO) by EH *i*
$C_e, C_g, C_{del}, C_{trading}$	Cost for purchasing electricity, gas, delivery cost and payment for trading
C_{op}	Operation cost of EH
$E_{1,i}^{t}, E_{2,i}^{t}, ...E_{15,i}^{t}$	Internal energy flow in EH *i*
$E_{out,e,i}^{t}, E_{out,h,i}^{t}, E_{out,g,i}^{t}$	Electricity, heat and gas output in EH *i*
$E_{in,e,i}^{t}, E_{in,g,i}^{t}$	Electricity, heat and gas input in EH *i*
$L_{h,i}^{t}, L_{e,i}^{t}, L_{g,i}^{t}$	Electricity, heat and gas load in EH *i*
$\Delta E_{hs,i}^{t}, \Delta E_{es,i}^{t}$	Energy change in electric and heat storage in EH *i*
$P_{pur,e,i,j}^{t}, P_{sel,e,i,j}^{t}$	Electricity purchased and sold for EH *i* from EH *j*
$State_{hs,i}^{t}, State_{es.i}^{t}$	Electric and heat storage state in EH *i*
$E_{hs,i}^{t}, E_{es,i}^{t}$	Energy of electric and heat storage in EH *i*
$\mu_{k,i}^{t}$	Continuous variable to guarantee the solution in the certain range
ψ_{ij}	Payment to node *j* by node *i* in energy trading

Constants and Sets:

G_{ij}, B_{ij}	Matrix of conductance and susceptance from node *i* to node *j*
G'_{ij}, B'_{ij}	Matrix of conductance and susceptance without shunt element from node *i* to node *j*
g_{ij}, b_{ij}	Conductance and susceptance from node *i* to node *j*
H, T, U, W	Submatrix of inverse matrix
r_l, x_l	Resistance and reactance of line *l*
$a_{c,0}, a_{c,1}, a_{c,2}$	Coefficients in polygonal inner-approximation method
λ_G^p, λ_G^q	Price for active and reactive power generation
$\lambda_{SVC}^q, \lambda_{CB}^q$	Reactive power price for SVC, CB
NL	Number of total transmission lines

NG	Number of generation units
NB	Number of bus
$NSVC$	Number of SVCs
NCB	Number of CBs
V_1	Voltage of reference bus
α	Coefficient of delivery cost in energy trading
$V_{i,\min}, V_{i,\max}$	Minimum and maximum of nodal voltage magnitude
$P_{i,\min}^{G}, P_{i,\max}^{G}$	Minimum and maximum output of active power generation
$Q_{i,\min}^{G}, Q_{i,\max}^{G}$	Minimum and maximum output of reactive power generation
$Q_{i,\min}^{SVC}, Q_{i,\max}^{SVC}$	Minimum and maximum output of SVC
$Q_{i,\min}^{CB}, Q_{i,\max}^{CB}$	Minimum and maximum output of CB
$P_{pur,e,i,DSO}^{\max}, P_{pur,g,i,DSO}^{\max}$	Maximum amount of electricity and gas purchased from DSO in EH i
σ_g^t	Price of natural gas
$\eta_{e,ch}, \eta_{e,dis}$	Efficiency of charging and discharging of electric energy storage
$\eta_{h,ch}, \eta_{h,dis}$	Efficiency of charging and discharging of heat energy storage
$\eta_{chp,e}, \eta_{chp,h}$	Efficiency of converting gas into electricity and heat in combined heat and power (CHP)
η_{EB}	Efficiency of converting electricity into heat in electricity boiler (EB)
$E_{es,i}^0, E_{hs,i}^0$	Initial electric energy and heat energy storage in EH i
$v_{k,i}^t, \omega_{k,i}^t$	Electricity and heat boundary point in CHP of EH i
$E_{ch,h,i}^{\max}, E_{dis,h,i}^{\max}$	Maximum amount of charging and discharging of heat energy storage in EH i
$E_{ch,e,i}^{\max}, E_{dis,e,i}^{\max}$	Maximum amount of charging and discharging of electric energy storage in EH i
$E_{es,i}^{\max}, E_{hs,i}^{\max}$	Maximum anount of energy of heat energy storage in EH i
M	Set of EHs that do not participate in energy trading
M'	Set of EHs that take part in energy trading

I. Introduction

With rapid power market competition, development application of distributed generation (DG) and demand response (DR), it is necessary to introduce price signal in a distribution system to promote flexibility and reliability of distribution system. With distribution power market, more potential of DG and DR can be released.

With distribution locational marginal price (DLMP), distribution system operator (DSO) will minimize generation cost and optimize network operation. Participants will be able to gain the most benefits by determining the marginal price throughout the distribution system [1]. As a reasonable price signal, DLMP is the key to stimulate flexible loads to ensure the secure operation of power system and alleviate congestion in the network [2].

With DLMP, the consumers at nodes can have the detailed price information and take part in DR actively [3], which can help reducing power loss, improving asset management and increasing consumers' profit [4]. In a distribution system, electrical vehicle (EV) is an important component and more and more EVs exist in the distribution system. Some researchers had studied the relationship between DLMP and EV [5][6]. With DLMP applied in the distribution system, the network congestion caused by EV charging can be alleviated [5]. EV

charging can be optimized based on DLMP [6]. Furthermore, DLMP can relieve congestion in the distribution system and improve social welfare [7]. Moreover, DLMP can be used in electricity trading, which helps optimizing operation and trading decision of energy entity at different nodes.

DLMP is a price which can be decomposed into three parts [8][9]. Typically, DLMP is decomposed into energy price, loss price and congestion price. Besides, DLMP has a relationship with nodal voltage support, which is expressed as cost for reactive power compensation to increase nodal voltage [10]. In [11], the author proposed the concept of independent marginal loss to calculate the location marginal price in the distribution system. In [12], DLMP was decomposed into energy price, loss price, voltage violation price and congestion price, and meanwhile, DLMP has active power and reactive power components. However, to the best of the authors' knowledge, the coupled effect of active power and reactive power is ignored and has not been addressed. In fact, nodal active power will influence reactive power flow and nodal reactive power will influence active power flow in a distribution system, hence loss price is coupled with nodal active and reactive power. Loss price is an important component of DLMP, which should be analyzed further.

Many methods have been studied to calculate DLMP. The classical method is Lagrange function [13]. Based on the optimization objective of DSO, DLMP of each node at distribution system is obtained by relaxing the system constraints and derivation by nodal power. Game theory is used to reduce the loss allocation based on DLMP [14]. In [15], the DLMP through quadratic programming was used to solve the multiple solution issue of the aggregator optimization. The Karush-Kuhn-Tucker (KKT) conditions and the unique solution of the aggregator optimization ensure that the centralized DSO optimization and the decentralized aggregator optimization converge. Duality analysis is used in problem formulation and second order cone program relaxation is to decompose DLMP [16]. Benders decomposition theory was utilized in economic formulation [17] [18]. Three-level networks were proposed in [17], including national (regional) transmission network, distribution network and local embedded networks or microgrids. Each network operator communicates its generalized bid functions (GBFs) to the next higher level network. Benders cuts are employed in simulating the GBFs. In [18], a distributed economic dispatch mechanism based on the modified Benders decomposition and distributed generation cost was proposed to reduce the dispatch complexity in facing high penetration of distributed energy resourses. In [19], DLMP was calculated based on the contribution of the DG to reduce the amount of loss and emission.

The direct current (DC) power flow model is easy to develop but it cannot evaluate reactive power and voltage in a distribution system. Meanwhile, the error of a DC model in a distribution system is not negligible. Hence DC power flow is not suitable for calculating DLMP in a distribution system. In [20], the authors proposed quadratic convex relaxation for AC optimal power flow, and compared the computational results with semi-definite programming (SDP) and second-order cone (SOC) relaxations. The above three relaxation methods are effective in calculating power flow model. However, DLMP is relevant to the derivative of operation constraints, such as total power balance, line capacity and nodal voltage limits. It is difficult to apply relaxation methods in modeling DLMP.

Although the traditional alternating current (AC) power flow considers the reactive power and evaluates the voltage level, this method decouples the active and reactive power. In fact, in high r/x ratio scenario, nodal active power will affect reactive power distribution and nodal reactive power will affect active power distribution. To the best of the authors' knowledge, reactive power delivery cost caused by nodal active power and active delivery cost caused by nodal reactive power have not been considered in the existing pricing mechanism. In this paper, linearized AC power flow model is used to develop sensitivity matrices to compose operation constraints which can then be adopted to formulate the DLMP model. Since the DLMP model is linear, DLMP can be decomposed into comprehensive components such as the energy price, loss price, congestion price and voltage support price. Meanwhile, DSO optimizes its economic dispatch and considers social welfare in DLMP calculation.

In the past few years, the day-ahead market has been paid much attention by researchers. When isolated systems cooperate and trade energy with each other, their schedule can be optimized and can benefit from trading [21]. An optimization-based framework for the optimal joint energy, reserve market and clearing algorithm was proposed in [22]. Mixed integer linear programming model and iterative approach were used to determine the optimal energy, reserves mix, the resulting market clearing prices, and calculate the welfares of the market participants. In [23], a linear programming based market clearing method in day-ahead electricity market was presented, with consideration of social welfare division among buyer and supplier.

Many methods are ultilized to clear P2P energy trading in a distribution network. In [24], multi-microgrids were traded in a distribution network by considering the reconfiguration of distribution network. Lagrange relaxation method was used to clear trading of multi-microgrids. In [25], multi-carrier energy systems were traded in reconfigurable distribution network. Cooperative game theory was ultilized to achieve maximal profit

of trading. Reference [26] proposed a bi-level model for transactive energy. The upper model was for the operation of distribution network, and the lower model was for multi-microgrid. In that model, distribution operator and each microgrid had independent objective function. The bi-level model was transformed into single layer model through Karush-Kuhn-Tucker (KKT) conditions. In [27], alternating direction method of multipliers (ADMM) were used to decompose operation problem of distribution network into sub-problem of distribution network and sub-problem of multi-microgrid. A blockchain-based double auction mechanism was proposed to simulate P2P energy trading in [28]. In [29], energy sharing mechanism was proposed, including residential photovoltaic (PV) as prosumer, and normal consumer. Leader-followers Stackelberg game theory was utilized to formulate a bi-level PV energy sharing problem, including the uncertainties of PV energy output, load demand, as well as electricity price. In [30], the optimal placement of suppliers' block bid in a day-ahead market was formulated as NP-hard combinatorial optimization problem to maximize the social welfare, which was solved by using genetic algorithm.

This paper proposes a novel electricity trading framework, in which EHs trade with each other considering their DLMPs in day-ahead market. In the DLMP model, based on linearized AC power flow and sensitivity matrices, DSO optimizes its economic dispatch, maximizes social welfare and clears DLMP for nodes in a distribution system. Moreover, DLMP is decomposed into comprehensive components for consumers, such as energy price, loss price, congestion price and voltage support price. Loss price caused by nodal active and reactive power is analyzed further. Consumers can have better understanding of price components and take further actions based on their DLMPs. Cooperative game theory is utilized in EH's trading model, considering the benefits of participants in trading. Trading benefits will be allocated by a fair manner. EHs can optimize their operation and trading decision based on their DLMPs.

The main contributions of this paper are as follows:

a) Based on linearized AC power flow, a novel DLMP model of coupled active and reactive power price is proposed by including five price components, i.e. energy price, loss price caused by nodal active power, loss price caused by nodal reactive power, congestion price and voltage support price. A detailed explanation with the experimental results about the loss price is provided;

b) Two power loss compensation terms are proposed with the inclusion of global compensation term and local compensation term. Global compensation term is used in the total power balance equations as operation constraints, which are vital to decompose DLMP. Local compensation term is used in calculating power flow of each line when using linearized power flow model based on sensitivity factors. Simulation results show the effectiveness of local compensation term.

c) After obtaining their DLMP information provided by DSO, EHs at different nodes can trade with each other based on DLMP and obtain their maximum profit. Cooperative game theory is used to model the trading process and the optimal trading result is solved by Nash bargaining. As shown later in the experimental result, EHs can benefit in trading with each other. The total cost is reduced by \$38.76 with a difference of 12.62%.

The rest of this paper is organized as follows. Section II presents linearized AC power flow model and sensitivity matrices. Section III proposes DLMP calculation and decomposition. Section IV presents the EH model. Case studies are used to demonstrate the effectiveness of the proposed method and chanllenges are discussed in Section V. Finally, Section VI concludes the paper. The detail proof of the two compensation terms is shown in the Appendix.

II. POWER FLOW AND SYSTEM SENSITIVITY MATRICES

The problem formulation is given as follows:

A. Linearized AC power flow equations

The linearized AC power flow in [31] is adopted to establish the DLMP model. The power flow equations are shown below:

$$P_{\mathrm{i}} = \sum_{j=1}^{n} G_{ij} V_j - \sum_{j=1}^{n} B'_{ij} \theta_j \tag{1}$$

$$Q_i = -\sum_{j=1}^{n} B_{ij} V_j - \sum_{j=1}^{n} G_{ij} \theta_j \tag{2}$$

$$PL_{ij} = g_{ij}(V_i - V_j) - b_{ij}(\theta_i - \theta_j) \tag{3}$$

$$QL_{ij} = -b_{ij}(V_i - V_j) - g_{ij}(\theta_i - \theta_j) \tag{4}$$

where the P_i and Q_i are injected active and reactive power at bus i, respectively. $Y_{ij} = G_{ij} + jB_{ij}$ is the i^{th} row and j^{th} column of the nodal admittance matrix Y. $Y'_{ij} = G'_{ij} + jB'_{ij}$ is the i^{th} row and j^{th} column of the nodal admittance matrix without shunt elements; $g_{ij} + jb_{ij}$ is the admittance of line (i, j). Generally, we assume that $G'_{ij} \approx G_{ij}$ since the shunt conductance is negligible compared with its susceptance in a distribution system.

B. Sensitivity matrices

Rewrite Equations (1) and (2) in the matrix form, for bus i,

$$\begin{bmatrix} P_i \\ Q_i \end{bmatrix} = \begin{bmatrix} G_{i,\cdot} & -B'_{i,\cdot} \\ -B_{i,\cdot} & -G_{i,\cdot} \end{bmatrix}_{2\times 2n} \begin{bmatrix} V \\ \theta \end{bmatrix}_{2n\times 1} \tag{5}$$

where the $G_{i,}$, $B'_{i,}$ and $B_{i,}$ are the i^{th} row of matrix $G = [G_{ij}]_{n\times n}$, $B' = [B'_{ij}]_{n\times n}$ and $B = [B_{ij}]_{n\times n}$, respectively. $V = [V_i]_{n\times 1}$ and $\theta = [\theta_i]_{n\times 1}$ are the vector of bus voltage magnitude and phase, respectively. $[*]_{i,\cdot}$ denotes the i^{th} row of matrix $[*]_{n\times n}$, which is a $n \times 1$ matrix. $[*]_{l,i}$ denotes the l^{th} row and i^{th} column element of matrix $[*]_{n\times n}$. $[*]_i$ denotes the i^{th} element of matrix $[*]_{n\times 1}$. The above three expressions are used in representing element and row for the matrix in Sections II and III.

Reformulate Equation (5) for all buses in the compact form, Equation (5) is transformed to

$$\begin{bmatrix} P \\ Q \end{bmatrix}_{2n\times 1} = \begin{bmatrix} G & -B' \\ -B & -G \end{bmatrix}_{2n\times 2n} \begin{bmatrix} V \\ \theta \end{bmatrix}_{2n\times 1} \tag{6}$$

Inverse the coefficient matrix of Equation (6), then

$$\begin{bmatrix} V \\ \theta \end{bmatrix}_{2n\times 1} = \begin{bmatrix} G & -B' \\ -B & G \end{bmatrix}^{-1}_{2n\times 2n} \begin{bmatrix} P \\ Q \end{bmatrix}_{2n\times 1} = \left[\begin{array}{c:c} H_{n\times n} & T_{n\times n} \\ \hdashline U_{n\times n} & W_{n\times n} \end{array}\right]^{-1}_{2n\times 2n} \begin{bmatrix} P \\ Q \end{bmatrix}_{2n\times 1} \tag{7}$$

where $H_{n\times n}, T_{n\times n}, U_{n\times n}$ and $W_{n\times n}$ are the submatrices of the inverse matrix.

1) Shift factors calculation

Similar to the concept of power transfer distribution factor (PTDF), sets of sensitivity matrices can be derived as follows:

$$SF_{v-p} = \frac{\partial V}{\partial P_i} = \frac{\partial (HP + TQ)}{\partial P} = H \tag{8}$$

$$SF_{v-q} = \frac{\partial V}{\partial Q_i} = \frac{\partial (HP + TQ)}{\partial Q} = T \tag{9}$$

$$SF_{\theta-p} = \frac{\partial \theta}{\partial P_i} = \frac{\partial (UP + WQ)}{\partial P} = U \tag{10}$$

$$SF_{\theta-q} = \frac{\partial \theta}{\partial Q_i} = \frac{\partial (UP + WQ)}{\partial Q} = W \tag{11}$$

where SF_{v-p} and SF_{v-q} are the $n \times n$ sensitivity matrix of nodal voltage magnitude changes *w.r.t.* nodal active and reactive power injections respectively. $SF_{\theta-p}$ and $SF_{\theta-q}$ are the $n \times n$ sensitivity matrix of nodal voltage phase changes *w.r.t.* nodal active and reactive power injections respectively. According to Equation (3),

$$\begin{aligned} \left[SF_{p-p}\right]_{l,\cdot} &= \frac{\partial PL_{ij}}{\partial P_i} = \frac{\partial \left(g_{ij}\left(V_i - V_j\right) - b_{ij}\left(\theta_i - \theta_j\right)\right)}{\partial P} \\ &= \frac{\partial \left(g_{ij}\left(H_{i,\cdot}P - T_{j,\cdot}P\right) - b_{ij}\left(U_{i,\cdot}P - U_{j,\cdot}P\right)\right)}{\partial P} \\ &= g_{ij}\left(H_{i,\cdot} - H_{j,\cdot}\right) - b_{ij}\left(U_{i,\cdot} - U_{j,\cdot}\right) \end{aligned} \tag{12}$$

$$\begin{aligned}\left[SF_{p-q}\right]_{l,\cdot} &= \frac{\partial PL_{ij}}{\partial Q_i} = \frac{\partial\left(g_{ij}\left(V_i - V_j\right) - b_{ij}\left(\theta_i - \theta_j\right)\right)}{\partial Q} \\ &= \frac{\partial\left(g_{ij}\left(T_{i,\cdot}Q - T_{j,\cdot}Q\right) - b_{ij}\left(W_{i,\cdot}Q - W_{j,\cdot}Q\right)\right)}{\partial Q} \\ &= g_{ij}\left(T_{i,\cdot} - T_{j,\cdot}\right) - b_{ij}\left(W_{i,\cdot} - W_{j,\cdot}\right)\end{aligned} \tag{13}$$

where SF_{p-p} and SF_{p-q} are the $n \times n$ sensitivity matrix of branch active flow changes *w.r.t.* nodal active and reactive power injections respectively. *i* and *j* are the start bus and end bus of line *l*, respectively. According to Equation (4),

$$\begin{aligned}\left[SF_{q-p}\right]_{l,\cdot} &= \frac{\partial QL_{ij}}{\partial P_i} = \frac{\partial\left(-b_{ij}\left(V_i - V_j\right) - g_{ij}\left(\theta_i - \theta_j\right)\right)}{\partial P} \\ &= -b_{ij}\left(H_{i,\cdot} - H_{j,\cdot}\right) - g_{ij}\left(U_{i,\cdot} - U_{j,\cdot}\right)\end{aligned} \tag{14}$$

$$\begin{aligned}\left[SF_{q-q}\right]_{l,\cdot} &= \frac{\partial QL_{ij}}{\partial Q_i} = \frac{\partial\left(-b_{ij}\left(V_i - V_j\right) - g_{ij}\left(\theta_i - \theta_j\right)\right)}{\partial Q} \\ &= -b_{ij}\left(T_{i,\cdot} - T_{j,\cdot}\right) - g_{ij}\left(W_{i,\cdot} - W_{j,\cdot}\right)\end{aligned} \tag{15}$$

where SF_{q-p} and SF_{q-q} are the sensitivity factors of branch reactive power flow changes *w.r.t.* nodal active and reactive power injections respectively.

2) Loss factors calculation

The loss factor (LF) and Factitious nodal demand (FND) models [32] are calculated to determine the power loss in the network. The LF at a bus shows how the system loss will change if the injection at the bus is changed by one unit.

The LF can be calculated as follows:

$$\begin{aligned}\left[LF_{p-p}\right]_i &= \frac{\partial PLoss}{\partial P_i} = \frac{\partial \sum_{l\in NL} r_l \cdot \left(\frac{PL_l^2 + QL_l^2}{V_l^2}\right)}{\partial P_i} \\ &\approx \sum_{l\in NL} \frac{r_l}{V_l^2}\left(2 \times PL_l \frac{\partial PL_l}{\partial P_i} + 2 \times QL_l \frac{\partial QL_l}{\partial P_i}\right) \\ &= \sum_{l\in NL} 2 \times \frac{r_l}{V_l^2}\left(PL_l\left[SF_{p-p}\right]_{l,i} + QL_l\left[SF_{q-p}\right]_{l,i}\right)\end{aligned} \tag{16}$$

$$\begin{aligned}\left[LF_{p-q}\right]_i &= \frac{\partial PLoss}{\partial Q_i} = \frac{\partial \sum_{l\in NL} r_l \cdot \left(\frac{PL_l^2 + QL_l^2}{V_l^2}\right)}{\partial Q_i} \\ &\approx \sum_{l\in NL} \frac{r_l}{V_l^2}\left(2 \times PL_l \frac{\partial PL_l}{\partial Q_i} + 2 \times QL_l \frac{\partial QL_l}{\partial Q_i}\right) \\ &= \sum_{l\in NL} 2 \times \frac{r_l}{V_l^2}\left(PL_l\left[SF_{p-q}\right]_{l,i} + QL_l\left[SF_{q-q}\right]_{l,i}\right)\end{aligned} \tag{17}$$

where LF_{p-p} and LF_{p-q} are the sensitivity matrices of system active power loss *w.r.t.* nodal active and reactive power injection respectively. $r_l + jx_l$ is the impedance of line *l*.

Similarly, the sensitivity matrices of system reactive power loss *w.r.t.* nodal active and reactive power injection are shown as follows:

$$\begin{aligned}\left[LF_{q-p}\right]_i &= \frac{\partial QLoss}{\partial P_i} = \frac{\partial \sum_{l\in NL} x_l \cdot \left(\frac{PL_l^2 + QL_l^2}{V_l^2}\right)}{\partial P_i} \\ &\approx \sum_{l\in NL} \frac{x_l}{V_l^2}\left(2\times PL_l \frac{\partial PL_l}{\partial P_i} + 2\times QL_l \frac{\partial QL_l}{\partial P_i}\right) \\ &= \sum_{l\in NL} 2\times \frac{x_l}{V_l^2}\left(PL_l\left[SF_{p-p}\right]_{l,i} + QL_l\left[SF_{q-p}\right]_{l,i}\right)\end{aligned} \tag{18}$$

$$\begin{aligned}\left[LF_{q-q}\right]_i &= \frac{\partial QLoss}{\partial Q_i} = \frac{\partial \sum_{l\in NL} x_l \cdot \left(\frac{PL_l^2 + QL_l^2}{V_l^2}\right)}{\partial Q_i} \\ &\approx \sum_{l\in NL} \frac{x_l}{V_l^2}\left(2\times PL_l \frac{\partial PL_l}{\partial Q_i} + 2\times QL_l \frac{\partial QL_l}{\partial Q_i}\right) \\ &= \sum_{l\in NL} 2\times \frac{x_l}{V_l^2}\left(PL_l\left[SF_{p-q}\right]_{l,i} + QL_l\left[SF_{q-q}\right]_{l,i}\right)\end{aligned} \tag{19}$$

where LF_{q-p} and LF_{q-q} are the sensitivity matrices of system reactive power loss *w.r.t.* nodal active and reactive power injection respectively.

It should be noted that shift factors only depend on parameter and topology of network. Loss factors have a relationship with shift factors and will change in different operation conditions.

C. Compensation terms

Two compensation terms have been proposed for power loss, namely global compensation term and local compensation term.

Global compensation term is used in the total power balance equations to ensure the total power balance. Global compensation term are $PLoss$ and $QLoss$ as shown in Equations (20) and (21) respectively. The total power balance equations are considered as constraints by DSO in the optimization problem, which is important in the derivation of DLMP.

$$\sum_{i=1}^{NB} P_i - LF_{p-p}\bullet P - LF_{p-q}\bullet Q + PLoss = 0 \tag{20}$$

$$\sum_{i=1}^{NB} Q_i - LF_{q-p}\bullet P - LF_{q-q}\bullet Q + QLoss = 0 \tag{21}$$

Local compensation terms are utilized in FND model to modify the power flow [32] . Local compensation terms are the third terms as shown in Equations (22) and (23).

$$PL_l = \sum_{i=1}^{NB}\left(\begin{array}{l}\left[SF_{p-p}\right]_{l,i}\bullet(P_i + F_i^p) + \left[SF_{p-q}\right]_{l,i}\bullet(Q_i + F_i^q) + \\ 0.25\times\left\{\begin{array}{l}\left[LF_{p-p}\right]_{l,i}\bullet(P_i + F_i^p) + \\ \left[LF_{p-q}\right]_{l,i}\bullet(Q_i + F_i^q)\end{array}\right.\end{array}\right) \tag{22}$$

$$QL_l = \sum_{i=1}^{NB}\left(\begin{array}{l}\left[SF_{q-p}\right]_{l,i}\bullet(P_i + F_i^p) + \left[SF_{q-q}\right]_{l,i}\bullet(Q_i + F_i^q) + \\ 0.25\times\left\{\begin{array}{l}\left[LF_{q-p}\right]_{l,i}\bullet(P_i + F_i^p) + \\ \left[LF_{q-q}\right]_{l,i}\bullet(Q_i + F_i^q)\end{array}\right.\end{array}\right) \tag{23}$$

The proof of the two compensation terms is detailed in the Appendix.

III. DLMP CALCULATION AND DECOMPOSITION

To clear the distribution system market, a DLMP model is proposed with linearized AC power flow. The objective of DSO is minimize the operation cost while satisfying the energy demand of each node and system

constraints. The objective function given in Equation (24) includes the cost of active and reactive power generation, static VAr compensators (SVCs) and capacitor banks (CBs).

Constraints (25) and (26) represent the constraints of total active and reactive power balance. Constraint (27) represents the limit of line capacity, which is linearized by a series of linear equations using a polygonal inner-approximation method. Constraint (28) represents the nodal voltage limit. Constraints (29)-(32) limit the output of the generatorsSVC and CB.

$$\min\ obj = \left(\sum_{i \in NG} (\lambda_G^p P_i^G + \lambda_G^q Q_i^G) + \sum_{i \in NSVC} \lambda_{SVC} Q_i^{SVC} + \sum_{i \in NCB} \lambda_{CB} Q_i^{CB} \right) \tag{24}$$

s.t.

$$\sum_{i=1}^{NB} P_i - LF_{p-p} \bullet P - LF_{p-q} \bullet Q + PLoss = 0 \quad (\eta_p) \tag{25}$$

$$\sum_{i=1}^{NB} Q_i - LF_{q-p} \bullet P - LF_{q-q} \bullet Q + QLoss = 0 \quad (\eta_q) \tag{26}$$

$$\begin{aligned} & a_{c,2} S_{\max} + a_{c,0} \left\{ \begin{array}{l} \sum_i [SF_{p-p}]_{i,:} (P + F^p) + \sum_i [SF_{p-q}]_{i,:} (Q + F^q) + \\ 0.25 \times \left\{ \begin{array}{l} \left[LF_{p-p} \right]_{l,i} \bullet (P_i + F_i^p) + \\ \left[LF_{p-q} \right]_{l,i} \bullet (Q_i + F_i^q) \end{array} \right. \end{array} \right. \\ & + a_{c,1} \left\{ \begin{array}{l} \sum_i [SF_{q-p}]_{i,:} (P + F^p) + \sum_i [SF_{q-q}]_{i,:} (Q + F^q) + \\ 0.25 \times \left\{ \begin{array}{l} \left[LF_{q-p} \right]_{l,i} \bullet (P_i + F_i^p) + \\ \left[LF_{q-q} \right]_{l,i} \bullet (Q_i + F_i^q) \end{array} \right. \end{array} \right. \end{aligned} \quad \forall l, (\eta_{l,c}) \tag{27}$$

$$V_{i,\min} \le V_1 + SF_{v-p}(P + F^p) + SF_{v-q}(Q + F^q) \le V_{i,\max} \quad (\eta_V^-, \eta_V^+) \tag{28}$$

$$P_{i,\min}^G \le P_i^G \le P_{i,\max}^G \quad (\eta_{PG}^-, \eta_{PG}^+) \tag{29}$$

$$Q_{i,\min}^G \le Q_i^G \le Q_{i,\max}^G \quad (\eta_{QG}^-, \eta_{QG}^+) \tag{30}$$

$$Q_{i,\min}^{SVC} \le Q_i^{SVC} \le Q_{i,\max}^{SVC} \quad (\eta_{SVC}^-, \eta_{SVC}^+) \tag{31}$$

$$Q_{i,\min}^{CB} \le Q_i^{CB} \le Q_{i,\max}^{CB} \quad (\eta_{CB}^-, \eta_{CB}^+) \tag{32}$$

where η_p, η_q, $\eta_{l,c}$, η_V^-, η_V^+, η_{PG}^-, η_{PG}^+, η_{QG}^-, η_{QG}^+, η_{SVC}^-, η_{SVC}^+, η_{CB}^- and η_{CB}^+ are the dual variables of the constraints.

The DLMP can be derived from the Lagrange function of the model (24)-(32). The Lagrange function is expressed as follows:

$$
\begin{aligned}
L = {} & obj - \eta_p \left(\sum_{i \in NB} P_i - LF_{p-p} \bullet P - LF_{p-q} \bullet Q + PLoss \right) - \eta_q \left(\sum_{i \in NB} Q_i - LF_{q-p} \bullet P - LF_{q-q} \bullet Q + QLoss \right) \\
& - \sum_{l \in NL} \sum_{\forall c} \eta_{l,c} \begin{pmatrix} \alpha_{c,0} S_{\max} + \\ \alpha_{c,1} \begin{pmatrix} \left[SF_{p-p} \right]_{l,i} \bullet \left(P_i + F_i^p \right) + \left[SF_{p-q} \right]_{l,i} \bullet \left(Q_i + F_i^q \right) + \\ 0.25 \times \left\{ \left[LF_{p-p} \right]_{l,i} \bullet \left(P_i + F_i^p \right) + \left[LF_{p-q} \right]_{l,i} \bullet \left(Q_i + F_i^q \right) \right\} \end{pmatrix} + \\ \alpha_{c,2} \begin{pmatrix} \left[SF_{q-p} \right]_{l,i} \bullet \left(P_i + F_i^p \right) + \left[SF_{q-q} \right]_{l,i} \bullet \left(Q_i + F_i^q \right) + \\ 0.25 \times \left\{ \left[LF_{q-p} \right]_{l,i} \bullet \left(P_i + F_i^p \right) + \left[LF_{q-q} \right]_{l,i} \bullet \left(Q_i + F_i^q \right) \right\} \end{pmatrix} \end{pmatrix} \\
& - \sum_{i \in NB} \eta_{V,i}^- \left(V_1 + \left[SF_{v-p} \right]_{i,\cdot} \bullet P_i + \left[SF_{v-q} \right]_{i,\cdot} \bullet Q_i - V_{i,\min} \right) - \sum_{i \in NB} \eta_{V,i}^+ \left(V_{i,\max} - \left(V_1 + \left[SF_{v-p} \right]_{i,\cdot} \bullet P_i + \left[SF_{v-q} \right]_{i,\cdot} \bullet Q_i \right) \right) \\
& - \sum_{i \in NG} \eta_{PG,i}^- \left(P_i^G - P_{i,\min}^G \right) - \eta_{PG}^+ \left(P_{i,\max}^G - P_i^G \right) - \sum_{i \in NG} \eta_{QG}^- \left(Q_i^G - Q_{i,\min}^G \right) - \eta_{QG}^+ \left(Q_{i,\max}^G - Q_i^G \right) \\
& - \sum_{i \in NSVC} \eta_{SVC}^- \left(Q_i^{SVC} - Q_{i,\min}^{SVC} \right) - \eta_{SVC}^+ \left(Q_{i,\max}^{SVC} - Q_i^{SVC} \right) - \sum_{i \in NCB} \eta_{CB}^- \left(Q_i^{CB} - Q_{i,\min}^{CB} \right) - \eta_{CB}^+ \left(Q_{i,\max}^{CB} - Q_i^{CB} \right)
\end{aligned} \tag{33}
$$

The first partial derivatives of Equation (33) *w.r.t.* the active and reactive power demand represent the active and reactive DLMP, respectively. Therefore, DLMPs are expressed as follows:

$$
\begin{aligned}
\sigma_k^p = \frac{\partial L}{\partial P_i} = {} & \eta_p - \left[LF_{p-p} \right]_k \eta_p - \left[LF_{q-p} \right]_k \eta_q \\
& + \sum_{\forall c} \sum_{l \in NL} \eta_{l,c} \begin{pmatrix} \alpha_{c1} \left(\left[SF_{p-p} \right]_{l,k} + 0.25 \times \left[LF_{p-p} \right]_{l,i} \right) + \\ \alpha_{c2} \left(\left[SF_{q-p} \right]_{l,k} + 0.25 \times \left[LF_{q-p} \right]_{l,i} \right) \end{pmatrix} \\
& + \sum_{i \in NB} \left(\eta_{V,i}^- - \eta_{V,i}^+ \right) \left[SF_{v-p} \right]_{i,\cdot k} \\
= {} & \sigma_{E,k}^p + \sigma_{Lp,k}^p + \sigma_{Lq,k}^p + \sigma_{Con,k}^p + \sigma_{Vs,k}^p
\end{aligned} \tag{34}
$$

$$
\begin{aligned}
\sigma_k^q = \frac{\partial L}{\partial Q_i} = {} & \eta_q - \left[LF_{p-q} \right]_k \eta_p - \left[LF_{q-q} \right]_k \eta_q \\
& + \sum_{\forall c} \sum_{l \in NL} \eta_{l,c} \begin{pmatrix} \alpha_{c1} \left(\left[SF_{p-q} \right]_{l,k} + 0.25 \times \left[LF_{p-q} \right]_{l,i} \right) + \\ \alpha_{c2} \left(\left[SF_{q-q} \right]_{l,k} + 0.25 \times \left[LF_{q-q} \right]_{l,i} \right) \end{pmatrix} \\
& + \sum_{i \in NB} \left(\eta_{V,i}^- - \eta_{V,i}^+ \right) \left[SF_{v-q} \right]_{i,\cdot k} \\
= {} & \sigma_{E,k}^q + \sigma_{Lp,k}^q + \sigma_{Lq,k}^q + \sigma_{Con,k}^q + \sigma_{Vs,k}^q
\end{aligned} \tag{35}
$$

For simplicity, the five terms in Equations (34) and (35) are represented by five variables as indicated. DLMP for active and reactive power is decomposed into five components, namely, energy price, power loss prices caused by nodal active and reactive power, congestion price and voltage support price. $\sigma_{E,k}^p$, $\sigma_{Lp,k}^p$, $\sigma_{Lq,k}^p$, $\sigma_{Con,k}^p$ and $\sigma_{Vs,k}^p$ represent the DLMP for active power of energy, power loss caused by nodal active and reactive power, congestion and voltage support respectively, while $\sigma_{E,k}^q$, $\sigma_{Lp,k}^q$, $\sigma_{Lq,k}^q$, $\sigma_{Con,k}^q$ and $\sigma_{Vs,k}^q$ represent the DLMP for reactive power for energy, power loss caused by nodal active and reactive power, congestion and voltage support, respectively.

It should be pointed out that the marginal active power injection will affect the reactive power price, while the marginal reactive power injection will affect the active power price. It is not accurate enough to decouple the active power and reactive power in clearing price with existing methods.

IV. EH MODEL FOR OPERATION AND TRADING

A. Structure of EH

Fig.1 shows the structure of EH, which includes combined heat and power (CHP), electric energy storage (ES), EB and heat energy storage (HS). CHP transforms gas into heat and electricity. ES stores electricity when the price is low and releases electricity when the price is high. EB is ulitilized to converting electricity into heat. HS stores the heat when the heat demand is low and releases the heat when the heat demand is high.

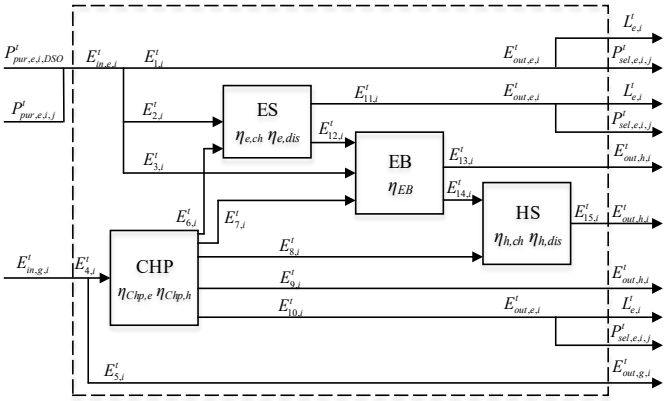

Fig. 1 Structure of EH

B. Operation constraints of EH

Constraints (36)-(66) represent the operation constraints of the proposed EH. Constraints (36)-(52) are the equality relationship among the variables of EH shown in Fig. 1. Since each branch in the proposed EH is given the energy flow direction, the input energy and the energy flow variables are positive in (51) and (52). Constraints (53) and (54) limit the input of CHP and EB respectively. Constraints (55) and (56) limit the input, output and the operation mode of HS respectively. HS is not allowed to store and release heat at the same time. Constraints (57) and (58) limit the capacity of HS. Constraints (59) and (60) limit the input, output and the operation mode of ES respectively. ES is not allowed to store and release electricity at the same time. Constraints (61) and (62) limit the capacity of ES. Constraints (63)-(66) are the operation constraints of CHP since the CHP output of electricity and heat are within a certain range [33].

$$E_{1,i}^t + E_{10,i}^t + E_{11,i}^t = E_{out,e,i}^t \tag{36}$$

$$E_{out,e,i}^t = P_{Load.i}^t + \sum_j P_{sel,e,i,j}^t \tag{37}$$

$$E_{out,h,i}^t = L_{h,i}^t \tag{38}$$

$$E_{out,g,i}^t = L_{g,i}^t \tag{39}$$

$$E_{5,i}^t = E_{out,g,i}^t \tag{40}$$

$$E_{9,i}^t + E_{13,i}^t + E_{15,i}^t = E_{out,h,i}^t \tag{41}$$

$$E_{1,i}^t + E_{2,i}^t + E_{3,i}^t = E_{in,e,i}^t \tag{42}$$

$$E_{4,i}^t + E_{5,i}^t = E_{in,g,i}^t \tag{43}$$

$$\eta_{h,ch} \bullet (E_{8,i}^t + E_{14,i}^t) - \eta_{h,dis} \bullet E_{15,i}^t = \Delta E_{hs,i}^t \tag{44}$$

$$\eta_{e,ch} \bullet (E_{2,i}^t + E_{6,i}^t) - \eta_{e,dis} \bullet E_{11,i}^t = \Delta E_{es,i}^t \tag{45}$$

$$\eta_{chp,e} \bullet E_{4,i}^t - E_{6,i}^t - E_{7,i}^t - E_{10,i}^t = 0 \tag{46}$$

$$\eta_{chp,h} \bullet E_{4,i}^t - E_{8,i}^t - E_{9,i}^t = 0 \tag{47}$$

$$\eta_{EB} \bullet (E_{3,i}^t + E_{7,i}^t + E_{12,i}^t) - E_{13,i}^t - E_{14,i}^t = 0 \tag{48}$$

$$E_{in,e,i}^t = P_{pur,e,i,DSO}^t + \sum_j P_{pur,e,i,j}^t \tag{49}$$

$$E_{in,g,i}^t = P_{pur,g,i}^t \tag{50}$$

$$E_{in,e,i}^t, E_{in,g,i}^t \geq 0, \forall i, \forall t \tag{51}$$

$$E_{1,i}^t, E_{2,i}^t, ..., E_{15,i}^t \geq 0, \forall i, \forall t \tag{52}$$

$$E_{4,i}^t \leq CHP_i^{\max}, \forall i, \forall t \tag{53}$$

$$E_{3,i}^t + E_{7,i}^t + E_{12,i}^t \leq EB_i^{\max} \tag{54}$$

$$E_{8,i}^t + E_{14,i}^t \leq \text{State}_{hs,i}^t \bullet E_{ch,h,i}^{\max}, \forall i, \forall t \tag{55}$$

$$E_{15,i}^t \leq (1 - \text{State}_{hs,i}^t) \bullet E_{dis,h,i}^{\max}, \forall i, \forall t \tag{56}$$

$$E_{hs,i}^{\min} \leq E_{hs,i}^t \leq E_{hs,i}^{\max} \tag{57}$$

$$E_{hs,i}^t = \begin{cases} E_{hs,i}^0 & if \ \ t = 0 \\ E_{hs,i}^{t-1} + \Delta E_{hs,i}^{t-1} & otherwise \end{cases} \forall i \tag{58}$$

$$E_{2,i}^t + E_{6,i}^t \leq \text{State}_{es,i}^t \bullet E_{ch,e,i}^{\max}, \forall i, \forall t \tag{59}$$

$$E_{11,i}^t + E_{12,i}^t \leq (1 - \text{State}_{es,i}^t) \bullet E_{dis,e,i}^{\max}, \forall i, \forall t \tag{60}$$

$$E_{es,i}^{\min} \leq E_{es,i}^t \leq E_{es,i}^{\max} \tag{61}$$

$$E_{es,i}^t = \begin{cases} E_{es,i}^0 & if \ \ t = 0 \\ E_{es,i}^{t-1} + \Delta E_{es,i}^{t-1} & otherwise \end{cases} \forall i \tag{62}$$

$$E_{6,i}^t + E_{7,i}^t + E_{10,i}^t = \sum_k \mu_{k,i}^t \bullet v_{k,i}^t \tag{63}$$

$$E_{8,i}^t + E_{9,i}^t = \sum_k \mu_{k,i}^t \bullet \omega_{k,i}^t \tag{64}$$

$$0 \leq \mu_{k,i}^t \leq 1, \quad \forall k, \forall i, \forall t \tag{65}$$

$$\sum_k \mu_{k,i}^t = 1, \quad \forall i, \forall t \tag{66}$$

C. Trading model of EH

1) Trading with DSO

$$0 \leq P_{pur,e,i,DSO}^t \leq P_{pur,e,i,DSO}^{\max} \tag{67}$$

$$0 \leq P_{pur,g,i,DSO}^t \leq P_{pur,g,i,DSO}^{\max} \tag{68}$$

$$C_g(P_{pur,g,i,D}^t) = \sum_{t=1}^{NT} \sigma_g^t \bullet P_{pur,g,i,DSO}^t \tag{69}$$

$$C_e(P_{pur,e,i,DSO}^t + Q_{pur,e,i,DSO}^t) = \sum_{t=1}^{NT} \left(\sigma_{P,i}^t \bullet P_{pur,e,i,DSO}^t + \sigma_{Q,i}^t \bullet Q_{pur,e,i,DSO}^t \right) \tag{70}$$

Constraints (67) and (68) represent the purchase limits of electricity and gas from DSO respectively. C_g and C_e denote the cost of purchasing gas and electricity from DSO respectively.

2) Trading with other EHs

EH at different nodes can trade with other EHs and optimize their schedule of energy supply for their demand. EHs will obtain optimal coordination to maximize their profit by Nash bargaining [34].

$$P_{pur,e,i,j}^t, P_{sel,e,i,j}^t \geq 0, \forall t, \forall i, j \in M, i \neq j \tag{71}$$

$$P_{pur,e,i,j}^t = P_{sel,e,j,i}^t, \forall t, \forall i, j \in M, i \neq j \tag{72}$$

$$\psi_{ij} = -\psi_{ji} \tag{73}$$

$$C_{trading}(\psi_{ij}) = \sum_{j \neq i} \psi_{ij} \tag{74}$$

$$C_{del}(P_{pur,e,i,j}^t) = \alpha \bullet (P_{pur,e,i,j}^t)^2 \tag{75}$$

Constraints (71) and (72) represent the limit in energy trading. The amount of electricity for purchasing and selling must be zero or positive. The amount of electricity purchased from *i* to *j* is equal to the amount sold from *j* to *i*. Constraint (73) shows the relationship of payment for trading. The sum of trading payment of buyer and seller is zero. The payment value can be zero, positive or negative. If the payment is positive, it means that the

participant should pay money in trading. Otherwise, the participant will receive money. Constraints (74) and (75) denote the payment and delivery cost in the EH trading respectively. The delivery cost is paid by the buyer in trading.

The operation cost includes the cost of purchasing power and gas from DSO and the delivery cost in EH trading.

$$\begin{aligned} &C_{op}(P^t_{pur,e,i,DSO}, Q^t_{pur,e,i,DSO}, P^t_{pur,g.i,DSO}, P^t_{pur,e,i,j}) \\ &= C_e(P^t_{pur,e,i,DSO}, Q^t_{pur,e,i,DSO}) + C_g(P^t_{pur,g.i,DSO}) + C_{del}(P^t_{pur,e,i,j}) \end{aligned} \tag{76}$$

C_{non} represents the operation cost at disagreement point, which means the operation cost when EHs do not trade with each other. EH will trade only if their total cost is less than C_{non}, which can be expressed as constraint (77).

$$C_{op}(P^t_{pur,e,i,DSO}, Q^t_{pur,e,i,DSO}, P^t_{pur,g.i,DSO}, P^t_{pur,e,i,j}) + C_{trading}(\psi_{ij}) \le C_{non} \tag{77}$$

The EHs take part in energy trading in order to maximize their profit.In this study, a cooperative game is proposed. The optimal trading will be indicated by the Nash equilibrium point, since each participant will optimize the trading strategy until the profits can be maximized. The Nash bargaining problem can be fumulated as follows:

$$\max \prod_{i \in M'} \left[C_{non} - (C_{op}(P^t_{pur,e,i,DSO}, Q^t_{pur,e,i,DSO}, P^t_{pur,g.i,DSO}, P^t_{pur,e,i,j}) + C_{trading}(\psi_{ij})) \right] \tag{78}$$

To reduce computational complexity, the bargaining problem is decomposed into two subproblem P1 and P2. P1 solves the energy schedule and trading decision of EHs, while P2 determines the payment of energy trading. EHs get extra benefit only when they take part in energy trading. According to [35][36], both P1 and P2 are convex.

P1: Operation cost minimization problem

$$\min \; C_{op}(P^t_{pur,e,i,DSO}, Q^t_{pur,e,i,DSO}, P^t_{pur,g.i,DSO}, P^t_{pur,e,i,j}) \tag{79}$$

We assume that EH cooperate to reduce their operation cost through trading. For EHs that do not trade, they will not get trading benefit and stop at P1. For EHs that take part in trading they will get trading benefit and continue to P2 to calculate their trading profit.

P2: Trading payment bargaining problem

$$\max \; \prod_{i \in M'} \left(\xi^* - C_{trading}(\psi_{ij}) \right) \tag{80}$$

where $\xi^* \triangleq C_{non} - C_{op}(P^t_{pur,e,i,DSO}, Q^t_{pur,e,i,DSO}, P^t_{pur,g.i,DSO}, P^t_{pur,e,i,j})$ represents the non-cooperative operation cost reduction based on optimal solution of P1.

V. Case Studies and Discussion

The effectiveness and validity of the proposed model is proved by utilizing the modified IEEE 33-bus system [37]. As depicted in Fig. 2, two generators are located at nodes 9 and 33, respectively. Two 300 kVAr SVCs are located at nodes 27 and 30, a 150 kVAr CB is located at node 12, and three 200 kVAr CBs are located at nodes 14, 18, and 32.

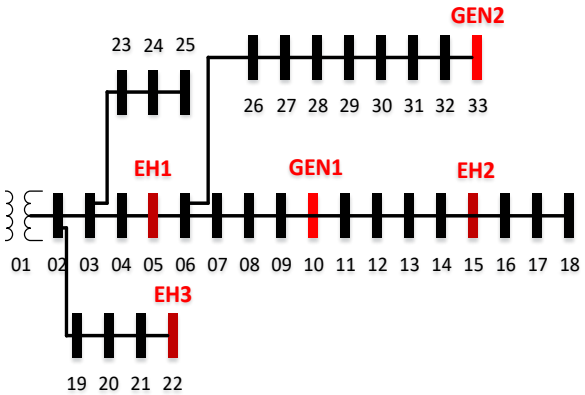

Fig. 2 The modified IEEE 33-bus system

To the best of the authors' knowledge, there is hardly any reactive power market so far. We set the reactive power price to 10% of the active power price [13]. The bidding price of the active power is set at 10 and 50 $/MWh for the substation GEN1 and GEN2 respectively. Accordingly, the reactive power price is set at 1 and

5 $/MVArh for the substation GEN1 and GEN2 respectively. Since GEN1 and GEN2 serve as backup generation, which will be used in peak load, the prices of GEN1 and GEN2 are higher than that of the substation. SVC and CB serve as reactive power compensation equipment and are installed in other nodes rather than in the substation. Hence the bidding prices of SVC and CB are higher than the reactive power price of the substation. The prices of SVC and CB are set as 1.5 and 1.4 $/MVArh respectively.

Here we consider three cases. Case 1 is to demonstrate the effetiveness of the proposed power flow model with a comparison of MATPOWER 6.0. Case 2 focuses on the DLMP and decomposition of DLMP. Case 3 is utilized to show the result of EH trading based on DLMP. All the cases are conducted on a Windows 10 64-bit personal computer with Intel Core i5-6500 3.2GHz CPU and 8 GB of RAM using MATLAB 2016b with Yalmip and Gurobi.

Case 1：Comparison of three power flow calculation methods

In Case 1, three methods are used to calculate the power flow, including 1) MATPOWER 6.0; 2) FND model without compensation term; 3) the proposed method. The results are shown in Fig. 3. The calculation of power flow by MATPOWER 6.0 is used as reference in this case. Compared with FND model without the compensation term, the proposed method brings less variation in both active and reactive power flows within an acceptable deviation. In a radial network, FND without the compensation term will result in a deviation of 50% line loss for each line, which will bring larger deviation in power flow.

Fig. 4 details the nodal imbalance of the two methods. The nodal imbalance shows the degree of imbalance between power flow and nodal supply or demand. The variation of power flow has a great impact on nodal imbalance. The proposed method also has less variation than the FND without compensation term in nodal imbalance, since the power flow calculated by the proposed method is more accurate than FND without compensation term.

Table I shows the nodal imbalance of different methods. The mean value of nodal imbalance of FND model is small, but the root mean square (RMS) is very large compared with the proposed method. The nodal imbalance of proposed method is small enough in this distribution system.

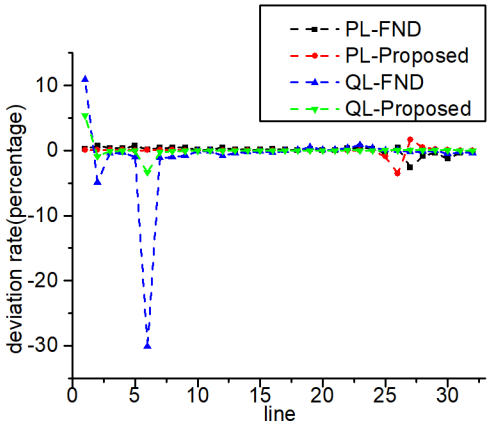

Fig. 3 Power flow deviation

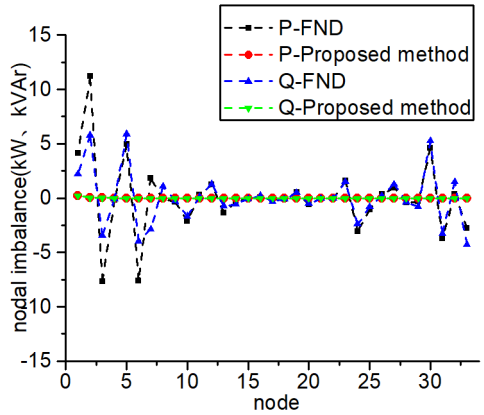

Fig. 4 Nodal imbalance

Table I Nodal imbalance of different methods

Method	FND model		Proposed method	
	P(kW)	Q(kVAr)	P(kW)	Q(kVAr)
Mean	3.5×10^{-4}	3.2×10^{-4}	3.3×10^{-4}	3.1×10^{-4}
RMS	3.2677	2.3744	3.82×10^{-2}	3.67×10^{-2}

Case 2：DLMP and decomposition of DLMP

Case 2 includes three scenarios: base load, valley load and peak load for the modified IEEE 33-bus system. DLMP consists of active power price and reactive power price. Each power price is decomposed into five components: energy price, loss price caused by active and reactive power, congestion price and voltage support price. Tables II, III and IV show the details of decomposition of DLMP under three loads. It should be noted that all these components are related to a dual multiplier of relative constraints.

Energy price is derived from the dual multiplier of power balance of the system, which is not always equal to the price of substation at node 1. Energy price depends on specific operating condition. When the load is a base load, the energy price of active power is 24.388 \$/MWh, which is not equal to the active power price of substation.

Figs. 5, 6 and 7 show each component of the loss price at all nodes except for node 1 in the three scenarios. The loss price is influenced by both nodal active and reactive powers. The loss price is the loss factor multiplied by dual multiplier of total power balance. We assume that the power flow is unidirectional radially, i.e. the power flow is from node 1 to nodes 18, 22, 25, and 33. The loss factor is negative when the direction of actual power flow is the same as assumed, which means that if the nodal power increases, it will aggravate the loss of system. And the loss factor is positive when the direction of actual power flow is the opposite, which means that if the nodal power increases, it will alleviate the loss of the system. However, for loss price, negative means that increasing nodal demand can alleviate the loss of the system and get payment, and positive means that increasing nodal demand can aggravate the loss of the system and pay for the increasing loss.

Loss price caused by active power is related to the active power price, while loss price caused by nodal reactive power is related to the reactive power price. When the load is peak load and valley load, the active power energy price is 10 \$/MWh while the active power energy price is 1 \$/MVArh. When the load is base load, the active power energy price is 24.388 \$/MWh while the active power energy price is 1 \$/MVArh. The difference of two energy price is great, which results in great difference of loss price.

Loss factor also has impact on loss price. Loss factor is determined by power flow and shift factor. Once the topology and parameter of network is fixed, shift factor will not change with load. Hence the actual power flow affects the loss price directly. The direction of actual active power flow is the same as assumed when the load is low. Since the active power is mainly supplied by substation at node 1 and the system is radial, the loss factor will increase with the node shifting to end node of lines, i.e. nodes 18, 22, 25, and 33. Accordingly, the price of the active power loss will increase with the same trend. The tendency of price of reactive power loss is the same when the load is low. However, when the load increases to peak load, due to economic dispatch, it is more economical to supply reactive power by GEN1, GEN2, SVCs, and CBs, which leads the actual reactive power flow to be opposite as we assumed. Hence the price of reactive power loss is negative.

The congestion price shows the extent of the line congestion and how much the customers should pay for the congestion. In this case, the line capacity is set to 3 MVA. When a line is in congestion, the power flow of this line reaches a maximum and more power should be supplied by other lines. When the load is low, the congestion price is low. When the load increase, more power is supplied by expensive generators. Hence, the congestion price increases with load increasing.

The voltage support price depends on the specific power flow. In the traditional model, the nodal voltage is mainly affected by the longitudinal component of voltage variation, i.e. $(PL_l \bullet r_l + QL_l \bullet x_l)/V_l$. Since r/x ratio is small in transmission system, nodal voltage level mainly depends on reactive power flow. In the proposed model, nodal voltage level is determined by nodal active and reactive power, and sensitivity matrices SF_{v-p} and SF_{v-q}, rather than just by the reactive power flow in the traditional model. Sensitivity matrices SF_{v-p} and SF_{v-q} are used to evaluate the impact of nodal demand on nodal voltage. Both nodal active and reactive powers have influence on nodal voltage level. Once the topology and parameter are determined, the sensitivity matrices SF_{v-p} and SF_{v-q} can be obtained and will not be changed with the operating conditions. The FND is added to the nodal load which is used to calculate the impact on nodal demand on nodal voltage. This means that the customer should pay for the voltage support caused by neighborhood line loss. In other words, the user pays for nodal reactive power compensation to maintain nodal voltage. Since the voltage support price is zero at nodes 5, 15 and 22, the voltage support price is not shown at Tables II, III and IV.

As discussed above, every component of DLMP is analyzed. For customers, they will have a better understanding of their electricity price, change their behavior and participate in a demand response program for

their interests. Furthermore, the decomposition of DLMP is helpful to promote a fair and transparent power market.

Table II DLMP in base load

Node	DLMP of active power ($/MWh)				
	σ_E^p	σ_{Lp}^p	σ_{Lq}^p	σ_{Con}^p	σ^p
5	24.388	1.156	0.024	23.551	49.119
15	24.388	2.932	0.084	23.551	50.955
22	24.388	0.393	0.013	23.551	48.345
Node	DLMP of reactive power ($/MVArh)				
	σ_E^q	σ_{Lp}^q	σ_{Lq}^q	σ_{Con}^q	σ^q
5	1	-0.298	-0.006	6.301	6.997
15	1	-1.186	-0.035	6.301	6.08
22	1	0.122	0.005	6.301	7.428

Table III DLMP in peak load

Node	DLMP of active power ($/MWh)				
	σ_E^p	σ_{Lp}^p	σ_{Lq}^p	σ_{Con}^p	σ^p
5	10	0.352	0.018	52.274	62.644
15	10	1.072	0.077	52.274	63.423
22	10	0.200	0.174	52.274	62.648
Node	DLMP of reactive power ($/MVArh)				
	σ_E^q	σ_{Lp}^q	σ_{Lq}^q	σ_{Con}^q	σ^q
5	1	-0.069	-0.004	14.004	14.931
15	1	-0.823	-0.064	14.004	14.117
22	1	0.075	0.007	14.000	15.082

Table IV DLMP in valley load

Node	DLMP of active power ($/MWh)				
	σ_E^p	σ_{Lp}^p	σ_{Lq}^p	σ_{Con}^p	σ^p
5	10	0.492	0.025	1.013	11.53
15	10	1.242	0.087	1.013	12.342
22	10	0.125	0.010	1.013	11.148
Node	DLMP of reactive power ($/MVArh)				
	σ_E^q	σ_{Lp}^q	σ_{Lq}^q	σ_{Con}^q	σ^q
5	1	0.131	0.067	0.272	1.47
15	1	0.128	0.008	0.272	1.408
22	1	0.051	0.004	0.272	1.327

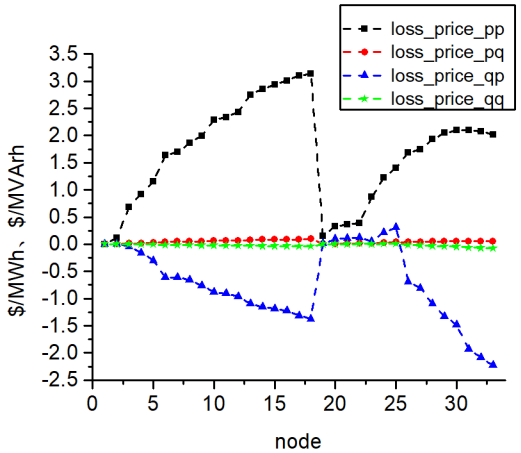

Fig.5 Loss price in base load

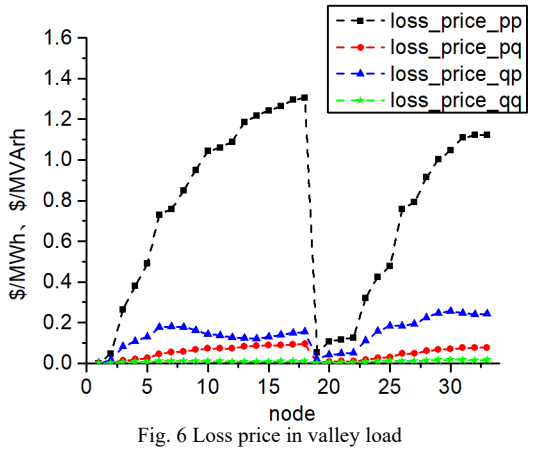

Fig. 6 Loss price in valley load

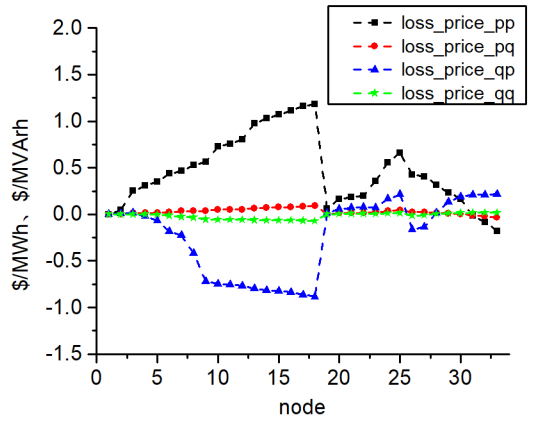

Fig. 7 Loss price in peak load

Case 3：EH trading based on DLMP

With energy trading, the EHs at different nodes will optimize their operation and trading decision based on DLMP determined by DSO. The 24-hours total active and reactive power load , active and reactive power price are depicted in Figs. 8 and 9. As shown in Figs. 8 and 9, both active and reactive powers price change with the similar trend of power load.

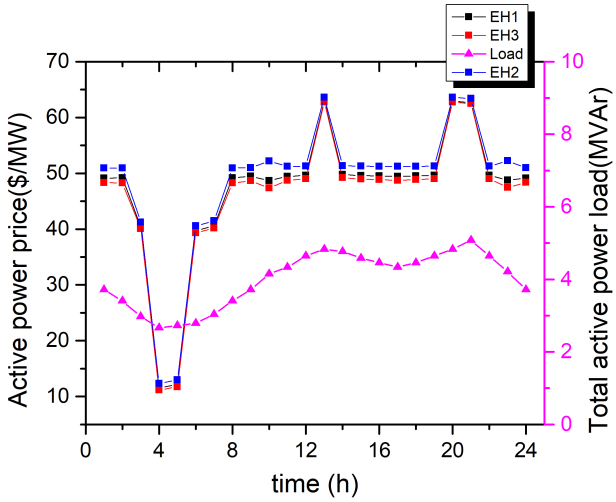

Fig. 8 Total active power load and active power price of EHs

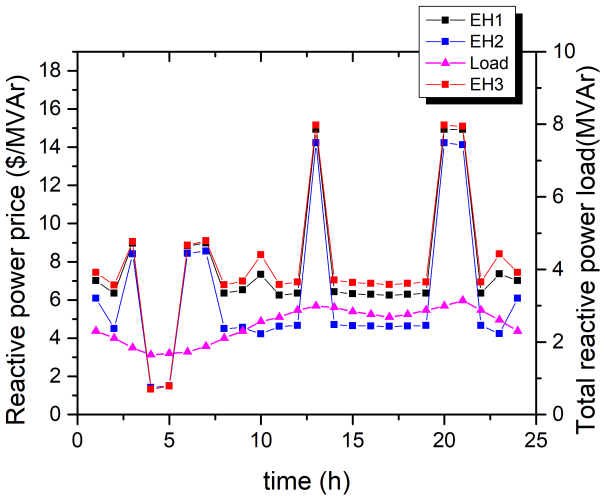

Fig. 9 Total reactive power laod and active power price of EHs

Table.V Cost and payment of EHs

	EH1	EH2	EH3	Total
Cost(no trading)($)	110.24	106.3	90.52	307.06
Cost(trading)($)	37.70	38.66	191.94	268.30
Payment(trading)($)	59.62	54.72	-114.34	0
Cost+payment(trading)($)	97.32	93.38	77.60	268.30

Table V shows the cost and payment of EHs. After energy trading, each EH obtains a profit of $12.92. The total cost is reduced by $38.76 and the difference is 12.62%.

The benefit is derived from two ways. First of all, with trading, EHs that locates at node with high LMP, will buy less electricity from DSO and trade more with other EHs with a bargaining way. EHs that locates at node with low LMP, will buy more electricity from DSO and sell electricity to other EHs. The change of electricity purchased from DSO is depicted in Figs. 10 (a) and (b). Secondly, the price of natural gas is set as about 2.8 $/Mbtu [38], which is equal to 9.55 $/MWh. The efficiency of CHP for converting gas into electricity is 40%. The price of electricity generated by CHP is 23.87 $/MWh. Except in the 4th and 5th hour, the price of electricity generated by CHP is less than LMP, hence more electricity is supplied by CHP. EH3 has larger load and larger scale of infrastructure. Hence EH3 can generate more electricity by its CHP and sell electricity to EH1 and EH2. Their total benefit can be obtained through energy trading.

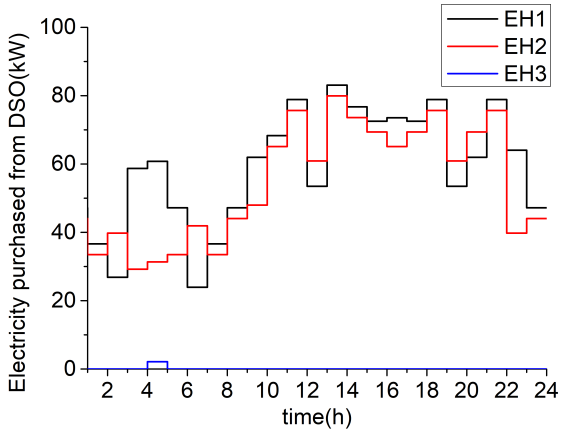

Fig. 10(a) Electricity purchased from DSO without EH trading

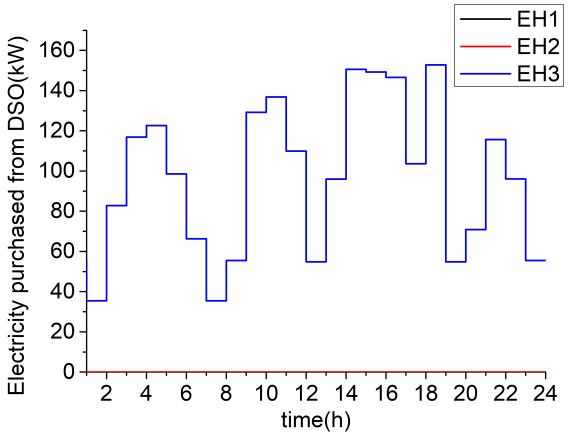

Fig. 10(b) Electricity purchased from DSO with EH trading

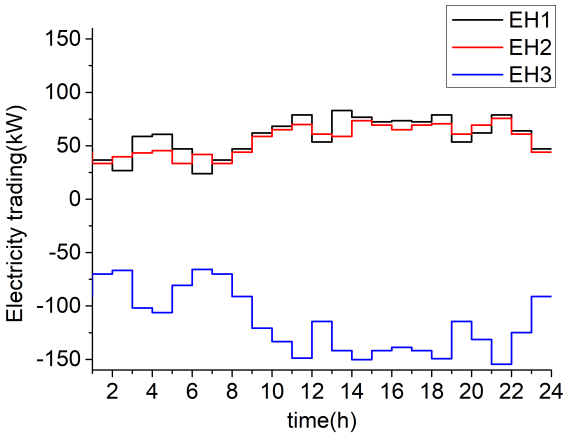

Fig.11 Electricity trading among EHs

As shown before, DLMP model is formulated based on specific load. Hence, DLMP is calculated hour-by-hour. In other words, DLMP calculation is repeated for 24 times. According to the simulation results, the maximum time in calculating DLMP for one hour is 402 seconds. In the present case study, the total time of calculating DLMP is 5969 seconds. For the EHs' trading process, it takes 58 seconds. Therefore the total time of simulation is 6027 seconds, and this is practically acceptable for the day-ahead market.

There are challenges in software implementation with many sensitivity matrices, constraints and equations involved. It is foreseen that the biggest challenge is to enhance the DLMP model for close-loop type distribution system. For example, electric vehicles and distributed renewable generations can take part in demand response based on DLMP.

VI. Conclusion

In this paper, a modified FND model based on linearized AC power flow is proposed. The model is verified with the modified IEEE 33-bus system. A local compensation term is added in FND model which enhances the calculation accuracy of the power flow and reduces the nodal power imbalance. DLMP for coupled active and reactive power in a distribution system is analyzed with three scenarios, i.e. base load, valley load and peak load. DSO will optimize the economic dispatch with different loads. DLMPs will change with different operating conditions. The energy price is derived by Lagrange multiplier which is determined by the operating conditions. The Lagrange multiplier is also used to determine the loss prices, congestion price and voltage support price which are influenced by the topology and parameters of the system. Nodal active and reactive power will affect both active and reactive power loss prices. In the given test system, the nodal active power has the larger effect than reactive power on loss price. Hence, the loss price caused by the active power is higher. The EHs at different nodes trade with each other using Nash bargaining. Through electricity trading, the EHs can reduce their operation costs and make profits. For example, each EH obtains a profit of $12.92 and the total cost is reduced by $38.76, a difference of 12.62%. The practicability to apply DLMP to large-scale distribution systems will be investigated in the future work.

ACKNOWLEDGMENTS

This work is sponsored in part by the Department of Finance and Education of Guangdong Province 2016 [202]: Key Discipline Construction Program, China; in part by the Education Department of Guangdong Province: New and Integrated Energy System Theory and Technology Research Group [Project Number 2016KCXTD022] and in part by the Brunel University London BRIEF Funding.

APPENDIX

A. Global compensation term

With the linearized AC power flow equations, the complex power loss is doubly calculated by the loss factors. The compensation terms $PLoss$ and $QLoss$ in Equations (A.3) and (A.4) are introduced to eliminate the overestimated active and reactive power loss, respectively. The rigorous proof of compensation term for active power loss is given below. For simplicity, the conclusion of compensation term of reactive power loss can be obtained by analogy.

$$\begin{aligned}
&\sum_{i=1}^{NB}\left(\left[LF_{p-p}\right]_i \bullet P_i + \left[LF_{p-q}\right]_i \bullet Q_i\right) \\
&= \sum_{i=1}^{NB}\begin{Bmatrix} \sum_{l\in NL} 2\times\frac{r_l}{V_l^2}\left(PL_l\left[SF_{p-p}\right]_{l,i} + QL_l\left[SF_{q-p}\right]_{l,i}\right)\bullet P_i + \\ \sum_{l\in NL} 2\times\frac{r_l}{V_l^2}\left(PL_l\left[SF_{p-q}\right]_{l,i} + QL_l\left[SF_{q-q}\right]_{l,i}\right)\bullet Q_i \end{Bmatrix} \\
&= \sum_{l\in NL}\frac{r_l}{\hat{V}_l^2}\begin{pmatrix} PL_l \bullet \sum_{i=1}^{NB}\left(\left[SF_{p-p}\right]_{l,i}\bullet P_i + \left[SF_{p-q}\right]_{l,i}\bullet Q_i\right) + \\ QL_l \bullet \sum_{i=1}^{NB}\left(\left[SF_{q-p}\right]_{l,i}\bullet P_i + \left[SF_{q-q}\right]_{l,i}\bullet Q_i\right) \end{pmatrix} \\
&= \sum_{l\in NL}\frac{r_l}{V_l^2}\left(PL_l^{\,2} + QL_l^{\,2}\right) = 2PLoss
\end{aligned} \tag{A.1}$$

$$\begin{aligned}
&\sum_{i=1}^{NB}\left(P_i - \left[LF_{p-p}\right]_i \bullet P_i - \left[LF_{p-q}\right]_i \bullet Q_i\right) \\
&= \sum_{i=1}^{NB} P_i - \sum_{i=1}^{NB}\left(\left[LF_{p-p}\right]_i \bullet P_i + \left[LF_{p-q}\right]_i \bullet Q_i\right) \\
&= PLoss - 2PLoss = -PLoss
\end{aligned} \tag{A.2}$$

Total active power balance equation can be formulated as below:

$$\sum_{i=1}^{NB} P_i - LF_{p-p}\bullet P - LF_{p-q}\bullet Q + PLoss = 0 \tag{A.3}$$

Similarly, total reactive power balance equation is written as below:

$$\sum_{i=1}^{NB} Q_i - LF_{q-p}\bullet P - LF_{q-q}\bullet Q + QLoss = 0 \tag{A.4}$$

B. Local compensation term

A case study is used to illustrate the necessity of compensation term in FND model when calculating the power flow. An example of active power loss is given. For simplicity, there is no demand at nodes. Ploss_i represents the power loss of line *i*.

The primary model is depicted as shown in Fig. 12 below:

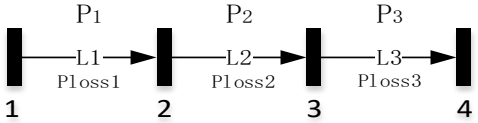

Fig. 12 Power flow in the primary model

The power flow of each line in the primary model is as follows:

$$\begin{bmatrix} P_1 \\ P_2 \\ P_3 \end{bmatrix} = \begin{bmatrix} 1 & 1 & 1 \\ 0 & 1 & 1 \\ 0 & 0 & 1 \end{bmatrix} \begin{bmatrix} Ploss_1 \\ Ploss_2 \\ Ploss_3 \end{bmatrix}$$

The FND model without compensation term is shown in Fig. 13.

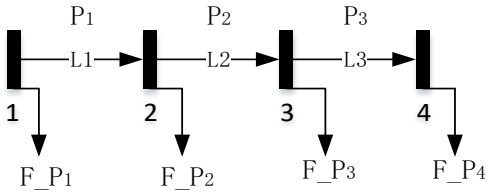

Fig.13 Power flow in FND without compensation

FND represents the power loss of the lines connected to a bus, which means that the power loss in each line is divided into two halves, attached to both buses of that line. Each half is represented as if it is an extra nodal demand [32].

The FND for each node are as follows:

$$\begin{bmatrix} F\_P_1 \\ F\_P_2 \\ F\_P_3 \\ F\_P_4 \end{bmatrix} = \frac{1}{2} \begin{bmatrix} 1 & 0 & 0 & 0 \\ 1 & 1 & 0 & 0 \\ 0 & 1 & 1 & 0 \\ 0 & 0 & 0 & 1 \end{bmatrix} \begin{bmatrix} Ploss_1 \\ Ploss_2 \\ Ploss_3 \\ Ploss_4 \end{bmatrix}$$

After utilizing the FND model, the power flow without actual demand at nodes is the sum of the FND of relative nodes. The power flow in FND model without compensation term is as follows:

$$\begin{bmatrix} P_1^{'} \\ P_2^{'} \\ P_3^{'} \end{bmatrix} = \begin{bmatrix} 1 & 1 & 1 \\ 0 & 1 & 1 \\ 0 & 0 & 1 \end{bmatrix} \begin{bmatrix} F\_P_2 \\ F\_P_3 \\ F\_P_4 \end{bmatrix} = \begin{bmatrix} 0.5 & 1 & 1 \\ 0 & 0.5 & 1 \\ 0 & 0 & 0.5 \end{bmatrix} \begin{bmatrix} Ploss_1 \\ Ploss_2 \\ Ploss_3 \end{bmatrix} \neq \begin{bmatrix} P_1 \\ P_2 \\ P_3 \end{bmatrix}$$

We can see that there is a variation of 50% of power loss for each line when calculating power flow using FND without compensation term. It should be pointed out that FND model is equivalent locally since the nodal power balance can be satisfied, but FND model is not equivalent globally since there is variation in power flow. However, FND is useful to calculate the nodal power impact on nodal voltage or power flow. Hence, when calculating the power flow, 50% of line power loss should be compensated for power flow.

In the proposed method, 50% of line power loss is compensated for power flow in FND model, as shown in the third terms of Equations (B.1) and (B.2). When the loss factor is used to calculate line loss, the coefficient should be multiplied by 0.5 according to Equation (A.1). The power flow equations in the proposed method are as follows:

$$PL_l = \sum_{i=1}^{NB} \left(\begin{array}{l} \left[SF_{p-p} \right]_{l,i} \bullet (P_i + F_i^p) + \left[SF_{p-q} \right]_{l,i} \bullet (Q_i + F_i^q) + \\ 0.25 \times \left\{ \begin{array}{l} \left[LF_{p-p} \right]_{l,i} \bullet (P_i + F_i^p) + \\ \left[LF_{p-q} \right]_{l,i} \bullet (Q_i + F_i^q) \end{array} \right. \end{array} \right) \tag{B.1}$$

$$QL_l = \sum_{i=1}^{NB} \left(\begin{array}{l} \left[SF_{q-p} \right]_{l,i} \bullet (P_i + F_i^p) + \left[SF_{q-q} \right]_{l,i} \bullet (Q_i + F_i^q) + \\ 0.25 \times \left\{ \begin{array}{l} \left[LF_{q-p} \right]_{l,i} \bullet (P_i + F_i^p) + \\ \left[LF_{q-q} \right]_{l,i} \bullet (Q_i + F_i^q) \end{array} \right. \end{array} \right) \tag{B.2}$$

REFERENCES

[1] J. Wei, L. Corson and A. K. Srivastava, "Three-phase Optimal Power Flow Based Distribution Locational Marginal Pricing and Associated Price Stability," 2015 IEEE Power & Energy Society General Meeting, Denver, CO, 2015, pp. 1-5.

[2] J. Zhao, Y. Wang, G. Song, P. Li, C. Wang and J. Wu, "Congestion Management Method of Low-voltage Active Distribution Networks Based on Distribution Locational Marginal Price," IEEE Access, vol. 7, 2019, pp. 32240-32255.

[3] F. Sahriatzadeh, P. Nirbhavane and A. K. Srivastava, "Locational Marginal Price for Distribution System Considering Demand Response," 2012 North American Power Symposium (NAPS), Champaign, IL, 2012, pp. 1-5.

[4] A. Mohsenzadeh and C. Pang, "Two Stage Residential Energy Management under Distribution Locational Marginal Pricing, " Electric Power Systems Research. 2018;154, pp.361-72.

[5] R. Li, Q. Wu and S. S. Oren, "Distribution Locational Marginal Pricing for Optimal Electric Vehicle Charging Management," IEEE Transactions on Power Systems, vol. 29, no. 1, Jan. 2014, pp. 203-211.

[6] Z. Liu, Q. Wu, S. S. Oren, S. Huang, R. Li and L. Cheng, "Distribution Locational Marginal Pricing for Optimal Electric Vehicle Charging through Chance Constrained Mixed-Integer Programming," IEEE Transactions on Smart Grid, vol. 9, no. 2, March 2018, pp. 644-654.

[7] M. Jafarian, J. Scherpen, K. Loeff, M. Mulder and M. Aiello, "A Combined Nodal and Uniform Pricing Mechanism for Congestion Management in Distribution Power Networks, " Electric Power Systems Research. 2020;180:106088.

[8] N. Steffan and G. T. Heydt, "Quadratic Programming and Related Techniques for the Calculation of Locational Marginal Prices in Distribution Systems," 2012 North American Power Symposium (NAPS), Champaign, IL, 2012, pp. 1-6.

[9] J. Hao, Y. Gu, Y. Zhang, J. J. Zhang and D. W. Gao, "Locational Marginal Pricing in the Campus Power System at the Power Distribution Level," 2016 IEEE Power and Energy Society General Meeting (PESGM), Boston, MA, 2016, pp. 1-5.

[10] S. Hanif, K. Zhang, C. M. Hackl, M. Barati, H. B. Gooi and T. Hamacher, "Decomposition and Equilibrium Achieving Distribution Locational Marginal Prices Using Trust-Region Method," IEEE Transactions on Smart Grid, vol. 10, no. 3, May 2019, pp. 3269-3281.

[11] J. -. Peng, H. Jiang, G. Xu, A. Luo and C. Huang, "Independent Marginal Losses with Application to Locational Marginal Price Calculation," IET Generation, Transmission & Distribution, vol. 3, no. 7, July 2009, pp. 679-689.

[12] M. Faqiry, L. Edmonds, H. Wu and A. Pahwa, " Distribution Locational Marginal Price-based Transactive Day-ahead Market with Variable Renewable Generation, " Applied Energy. 2020;259:114103.

[13] L. Bai, J. Wang, C. Wang, C. Chen and F. Li, "Distribution Locational Marginal Pricing (DLMP) for Congestion Management and Voltage Support," IEEE Transactions on Power Systems, vol. 33, no. 4, July 2018, pp. 4061-4073.

[14] K. Shaloudegi, N. Madinehi, S. H. Hosseinian and H. A. Abyaneh, "A Novel Policy for Locational Marginal Price Calculation in Distribution Systems Based on Loss Reduction Allocation Using Game Theory," IEEE Transactions on Power Systems, vol. 27, no. 2, pp. May 2012, pp. 811-820.

[15] S. Huang, Q. Wu, S. S. Oren, R. Li and Z. Liu, "Distribution Locational Marginal Pricing through Quadratic Programming for Congestion Management in Distribution Networks," IEEE Transactions on Power Systems, vol. 30, no. 4, July 2015, pp. 2170-2178.

[16] A. Papavasiliou, "Analysis of Distribution Locational Marginal Prices," IEEE Transactions on Smart Grid, vol. 9, no. 5, Sept. 2018, pp. 4872-4882.

[17] Z. Yuan, M. R. Hesamzadeh and D. R. Biggar, "Distribution Locational Marginal Pricing by Convexified ACOPF and Hierarchical Dispatch," IEEE Transactions on Smart Grid, vol. 9, no. 4, July 2018, pp. 3133-3142.

[18] Z. Yuan and M. Reza Hesamzadeh, "A Distributed Economic Dispatch Mechanism to Implement Distribution Locational Marginal Pricing," 2018 Power Systems Computation Conference (PSCC), Dublin, 2018, pp. 1-7.

[19] Azad-Farsani E, Agah SMM, Askarian-Abyaneh H, et al, "Stochastic LMP (Locational marginal price) Calculation Method in Distribution Systems to Minimize Loss and Emission Based on Shapley Value and Two-point Estimate Method, " Energy. 2016;107, pp. 396-408.

[20] C. Coffrin, H. L. Hijazi and P. Van Hentenryck, "The QC Relaxation: A Theoretical and Computational Study on Optimal Power Flow," IEEE Transactions on Power Systems, vol. 31, no. 4, July 2016, pp. 3008-3018.

[21] N. Koltsaklis, I. Gioulekas, M. Georgiadis, "Optimal Scheduling of Interconnected Power Systems," Computers & Chemical Engineering. 2018;111, pp. 164-82.

[22] N. Koltsaklis, A. Dagoumas, "Incorporating Unit Commitment aspects to the European Electricity Markets Algorithm: An Optimization Model for the Joint Clearing of Energy and Reserve Markets, " Applied Energy, 2018;231, pp.235-58.

[23] D. Shah and S. Chatterjee, " Improvement in Social Welfare Division among Buyer and Supplier in LP Based Market Clearing Method in Day-ahead Electricity Market, " Australian Journal of Electrical and Electronics Engineering, 2019.16:4, pp. 237-249

[24] Y. Wang, Z. Huang, M. Shahidehpour, L. L. Lai, Z. Wang and Q. Zhu, "Reconfigurable Distribution Network for Managing Transactive Energy in a Multi-Microgrid System," IEEE Transactions on Smart Grid, vol. 11, no. 2, March 2020, pp. 1286-1295. DOI 10.1109/TSG.2019.2935565

[25] Y. Wang, Z. Huang, Z. Li, et al. "Transactive Energy Trading in Reconfigurable Multi-carrier Energy Systems," Journal of Modern Power system and Clean Energy, vol. 8, no. 1, January 2020, pp. 67-76.

[26] Z. Wang, B. Chen, J. Wang, et al. "Coordinated Energy Management of Networked Microgrids in Distribution Systems, " IEEE Transactions on Smart Grid, 2015, 6(1), pp. 45-53.

[27] H. Gao, J. Liu, L. Wang, et al. "Decentralized Energy Management for Networked Microgrids in Future Distribution Systems," IEEE Transactions on Power Systems, 2017, 33(4), pp. 3599-3610.

[28] B.P. Hayes, S. Thakur, and J.G. Breslin, "Co-simulation of Electricity Distribution Networks and Peer to Peer Energy Trading Platforms,"International Journal of Electrical Power & Energy Systems,vol. 115,2020,105419

[29] X. Xu, J. Li, Y. Xu, Z. Xu and C. S. Lai, "A Two-stage Game-theoretic Method for Residential PV Panels Planning Considering Energy Sharing Mechanism," IEEE Transactions on Power Systems, DOI: 10.1109/TPWRS.2020.2985765

[30] D. Shah and S. Chatterjee, "Optimal Placement of Time Flexible Supplier's Block Bid in a Day-Ahead Electric Market Using Genetic Algorithm," 2019 Second International Conference on Advanced Computational and Communication Paradigms (ICACCP), Gangtok, India, IEEE, 2019, pp. 1-8

[31] J. Yang, N. Zhang, C. Kang and Q. Xia, "A State-Independent Linear Power Flow Model with Accurate Estimation of Voltage Magnitude," IEEE Transactions on Power Systems, vol. 32, no. 5, Sept. 2017, pp. 3607-3617.

[32] F. Li and R. Bo, "DCOPF-Based LMP Simulation: Algorithm, Comparison with ACOPF, and Sensitivity," IEEE Transactions on Power Systems, vol. 22, no. 4, Nov. 2007, pp. 1475-1485.

[33] X. Chen, C. Kang, M. O'Malley,et al. "Increasing The Flexibility of Combined Heat and Power for Wind Power Integration in China: Modeling and Implications," IEEE Transactions on Power Systems, vol. 30, no. 4, Jul. 2015, pp. 1848-1857.

[34] H. Wang and J. Huang, "Incentivizing Energy Trading for Interconnected Microgrids," IEEE Transactions on Smart Grid, vol. 9, no. 4, July 2018, pp. 2647-2657.

[35] S. Boyd and L. Vandenberghe, "Convex Optimization," Cambridge University Press, 2004

[36] J. F. Nash Jr, "The Bargaining Problem," Econometrica: Journal of the Econometric Society, 1950, pp. 155-162.

[37] M. E. Baran and F. F. Wu, "Network Reconfiguration in Distribution Systems for Loss Reduction and Load Balancing," IEEE Transactions on Power Delivery, vol. 4, no. 2, April 1989, pp. 1401-1407.

[38] Investing.com, 14th Sept. 2018. [Online] https://cn.investing.com/commodities/natural-gas.